



ELSEVIER

Journal of Alloys and Compounds 309 (2000) 127–131

Journal of
ALLOYS
AND COMPOUNDS

www.elsevier.com/locate/jallcom

The structure of the trihydride GdH_3

M. Ellner*, H. Reule, E.J. Mittemeijer

^aMax Planck Institute for Metals Research, Seestraße 92, D-70174 Stuttgart, Germany

Received 12 May 2000; accepted 29 May 2000

Abstract

The unit cell parameters of the trihydride GdH_3 (Pearson symbol $hP24$, space group $P\bar{3}c1$, HoH_3 type) were determined employing Guinier powder diffraction patterns. The structure of the interstitial compound GdH_3 is formed by departing from a hexagonal close-packed substructure of gadolinium and by filling its tetrahedral and triangular atomic positions with hydrogen atoms. The occupation of interstitial atomic positions in the hexagonal close-packed structure causes lattice dilatation associated with a significant change of the axial ratio c/a . In the intermediate phases of the binary system Gd-H , the interatomic distance between gadolinium and hydrogen atoms, $d_{\text{Gd-H}}$, decreases with increasing hydrogen content; the shortest $d_{\text{Gd-H}}$ distance was observed to occur in GdH_3 . A set of powder diffraction data was obtained for GdH_3 . © 2000 Elsevier Science S.A. All rights reserved.

Keywords: GdH_3 ; HoH_3 -type representatives; Interstitial compounds

1. Introduction

In the hydrogen-rich portion of the binary phase diagram Gd-H , two intermediate phases occur: The dihydride GdH_2 ($0.64 < x_H < 0.70$; with x_H = mole fraction of hydrogen; stable below 875 K) and the trihydride GdH_3 ($0.74 < x_H < 0.75$; stable below 875 K) [1]. The crystal structure of GdH_2 is isotopic with CaF_2 ($cF12$, $Fm\bar{3}m$, $a = 5.303 \text{ \AA}$) [2]. The outcome of the first investigation on the crystal structure of GdH_3 [2] was a proposed structure isotypical with PuH_3 ($hP8$, $P6_3/mmc$, $a = 3.73(1)$, $c = 6.71(2) \text{ \AA}$) [3]. PuH_3 is a representative of the Na_3As type structure [4]. A later neutron diffraction study on the crystal structure of the late RE-containing trihydrides (RE=rare earth) suggested that the structure of GdH_3 is isotypical with HoH_3 ($hP24$, $P\bar{3}c1$, $a = 6.46 \text{ \AA}$, $c = 6.71 \text{ \AA}$) [5,6]. Until now powder diffraction data have not been presented either for GdH_3 or for the other rare earth-containing representatives of the HoH_3 type structure [7]. This study provides such data and has been made as part of an investigation on the binary system Gd-H [8].

2. Experimental

The trihydride GdH_3 was prepared starting from gadolinium (purity 99.9 wt.%; Rhône-Poulenc). Bulk gadolinium ingots were hydrogenated by exposing them to a H_2 atmosphere (99.999 vol.%; Messer Griesheim) of 0.13 MPa at 775 K for 3 h and slowly cooling down to room temperature which yielded the composition $\text{GdH}_{3.1(1)}$ as determined by means of a desorption method that is carried out as follows [cf. Ref. [9]]. The samples are placed in a high-vacuum system which can be heated up to 975 K at the position of the sample using a radiation furnace. The vacuum system is operated by a turbo molecular pump having a constant pumping rate at pressures between 10^{-9} and 10^{-2} Pa. Hydrogen desorbs from the sample and is detected by a computer controlled mass spectrometer. A calibration of this device showed that the hydrogen concentration can be determined with a maximum relative error of 3%.

The bulk specimens were ground in a mortar under an argon atmosphere and subsequently passed through a sieve (mesh size: 0.05 mm). The particles which passed the sieve were used for the powder diffraction analysis. Powder diffraction patterns were recorded in a Guinier transmission camera (Enraf-Nonius FR552) using $\text{CuK}\alpha_1$ ($\lambda =$

*Corresponding author.

E-mail address: ellner@mf.mpi-stuttgart.mpg.de (M. Ellner).

Table 1
Powder diffraction data of the trihydride GdH_3^a

$(hkl)_h$	$(hkl)_H$	d_c [Å]	d_o [Å]	I_o	I_c
002	002	3.3585	3.3576	21	30
010	110	3.2331	3.2355	25	23
011	111	2.9132	2.9158	100	100
012	112	2.3292	2.3229	12	17
110	300	1.8667	1.8680	29	18
013	113	1.8407	1.8411	20	26
004	004	1.6793	–	–	4
112	032	1.6316	1.6315	20	24
020	220	1.6166	–	–	3
021	221	1.5717	1.5727	9	16
014	114	1.4902	–	–	5
022	222	1.4566	–	–	4
023	223	1.3107	1.3107	3	9
114	034	1.2484	1.2484	5	11
015	115	1.2406	1.2405	3	8
120	140	1.2220	–	–	3
121	141	1.2023	1.2020	7	15

^a $(hkl)_h$ = indexing of the $hP8$ unit cell ($\text{PuH}_3/\text{Na}_3\text{As}$ type); $(hkl)_H$ = indexing of the $hP24$ unit cell (HoH_3 type); c = calculated values; o = observed values.

1.540562 Å) radiation. Silicon (99.999999 wt.%; Ventron) was used as an internal calibration standard. The powdered specimens were put on a piece of adhesive band and were protected by a fine collodion film to prevent sample decomposition by atmospheric humidity. As another protection method to avoid such sample decomposition, diffraction measurements were also made using the airtight Guinier capillary technique. Single coated CEA Reflex 15 film was used for the Guinier photographs. The unit cell parameters were refined by least squares fitting of Bragg's equation to diffraction lines in the range $26^\circ < 2\theta < 80^\circ$.

Integrated intensities of diffraction lines recorded in the Guinier patterns were densitometrically analysed on the Line Scanner LS 20 (KEJ Instruments).

3. Results

By means of X-ray diffraction analysis, as compared with neutron diffraction analysis, complete information about the ordering of the lightest element hydrogen in the trihydride GdH_3 cannot be obtained. Thus, the Guinier patterns with $\text{CuK}\alpha_1$ radiation of the $\text{GdH}_{3.1(1)}$ specimens, obtained by application of either of both protection methods (indicated in Section 2), showed only diffraction lines of the $\text{PuH}_3/\text{Na}_3\text{As}$ structure type ($hP8$, $P6_3/mmc$) and not those of the HoH_3 structure type ($hP24$, $P\bar{3}c1$) which superstructure is formed by small displacements of hydrogen atoms. The least squares refined unit cell parameters obtained from the diffraction pattern are: $a = 3.7333(5)$ Å, $c = 6.717(3)$ Å and thus $c/a = 1.7992$. With reference to the structure determined for HoH_3 by neutron diffraction analysis [5,6], the powder diffraction data of GdH_3 shown in Table 1 can also be interpreted on the basis of the structure type HoH_3 . The corresponding least squares refined unit cell parameters are: $a = 6.4662(9)$ Å, $c = 6.717(3)$ Å and thus $c/a = 1.0388$.

The indices $(hkl)_h$ in Table 1 refer to the $hP8$ -substructure unit cell ($\text{PuH}_3/\text{Na}_3\text{As}$ type); the $(hkl)_H$ -indexing corresponds to the $hP24$ -superstructure unit cell (HoH_3 type). For the calculation of the powder diffraction intensities the program LAZY-PULVERIX [10] and the structure data for the HoH_3 type given in Ref [11] were used.

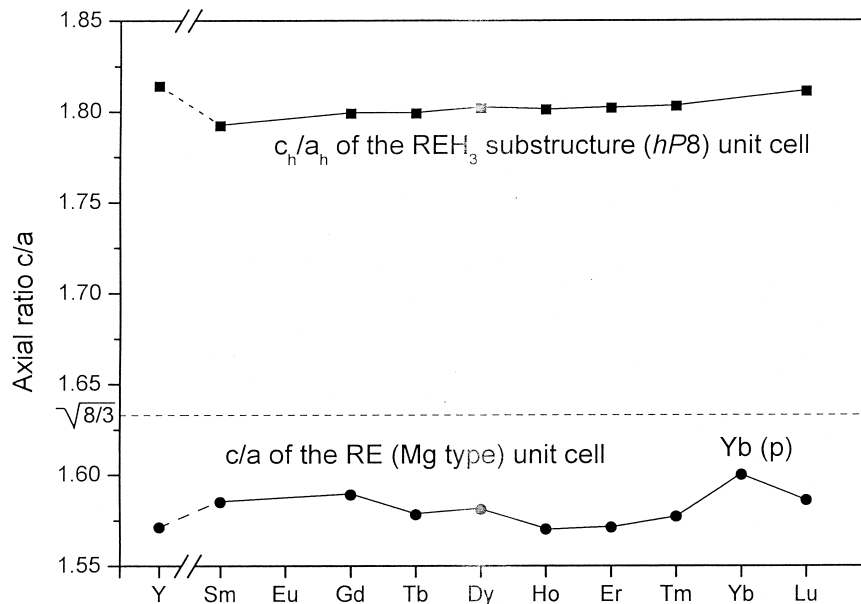


Fig. 1. Axial ratios c/a for the unit cell of yttrium and late RE-elements (Mg type) as well as (c_h/a_h) for the substructure-unit cell (Na_3As type) of the late RE-containing trihydrides REH_3 as function of atomic number Z (data from Ref. [4]).

No substantial change for the X-ray powder diffraction intensities is observed by the calculation on basis of the PuH_3 substructure.

4. Discussion

The crystal structures of phases occurring in the binary system Gd–H below 1500 K can be characterized by two common structural families: the Mg family (pertaining to solid solution $\alpha\text{-Gd}(\text{H})$ and the trihydride GdH_3) and the Cu family (pertaining to the dihydride GdH_2). In these binary phases, gadolinium occupies the atomic positions of the Mg or Cu structure type. The complete structure of the hydrogen-containing phases is then formed by full or partial occupation of tetrahedral, triangular and octahedral interstices of the Mg or Cu type structure by hydrogen. The defect CaF_2 structure of the dihydride GdH_2 has been described previously by the filling of tetrahedral interstitial sites of the Cu type structure by hydrogen, for the compositions $x_{\text{H}} \leq 2/3$, and by an additional partial filling of the octahedral interstitial sites by hydrogen for the compositions $x_{\text{H}} > 2/3$ [8]. In this study, the occupation by hydrogen of triangular and tetrahedral interstitial sites of the Mg type structure will be discussed for the trihydride GdH_3 .

The occupation of interstitial sites in the Mg type structure in general causes lattice dilatations associated with a significant change of the axial ratio c/a . Lattice dilatations as indicated are not the only possible cause for change of the axial ratio c/a : electronic effects can also contribute to its variation. Yttrium and the late rare earth elements — samarium . . . lutetium — are representatives of the Mg structure type. The electronic structure of these RE elements, characterized by the filling of the 4f band by electrons, influences the values of the axial ratio c/a as well (cf. the axial ratios c/a for the late rare earth elements as function of the atomic number shown in Fig. 1).

4.1. Relationship between the structure of the late RE elements (Mg type) and the substructure of the trihydrides REH_3 (Na_3As type)

Comparing the structure of the trihydride GdH_3 (HoH₃ type) with that of the late rare earth element modification $\alpha\text{-Gd}$ (Mg type, $P6_3/mmc$, 2Gd (c); [12]), it follows that the GdH_3 structure can be derived in two steps: (i) By filling of the triangular (2b) and the tetrahedral (4f) atomic positions of the gadolinium sublattice with hydrogen resulting in the $\text{Na}_3\text{As}/\text{PuH}_3$ type structure ($P6_3/mmc$, 2Gd (c); 2H (b); 4H (f) $z=0.607$) [11,13]; (ii) by subsequent displacement of the hydrogen atoms occupying the fourfold atomic position 4(f). These realize the HoH₃ type structure [11] with a three times larger unit cell.

It is striking that the the hydrogen-containing representatives of the HoH₃ structure type are formed only by the

late rare earth elements which crystallize themselves in the Mg structure. The axial ratio c/a of yttrium and that of the late RE ($4f^6 \dots 4f^{14}$) elements isotypical with Mg is shown at the bottom part of Fig. 1. These late RE elements show values of the axial ratio c/a smaller than the ideal close-packed value of $\sqrt{8/3}$. (The relatively high c/a -value of ytterbium originates from the high-pressure Yb-modification that is stable at 30.9 GPa [14]). The axial ratios c_h/a_h (the subscript h refers to the Na_3As type structure unit cell; cf. section 4.2) for the late RE-containing trihydrides REH_3 , are given in the upper part of Fig. 1. These axial ratios c_h/a_h are significantly larger than the ideal c/a -axial ratio of the hexagonal close-packed structure [$\sqrt{8/3}$].

For pure $\alpha\text{-Gd}$ [$c/a=1.590 < \sqrt{8/3}$], a schematic

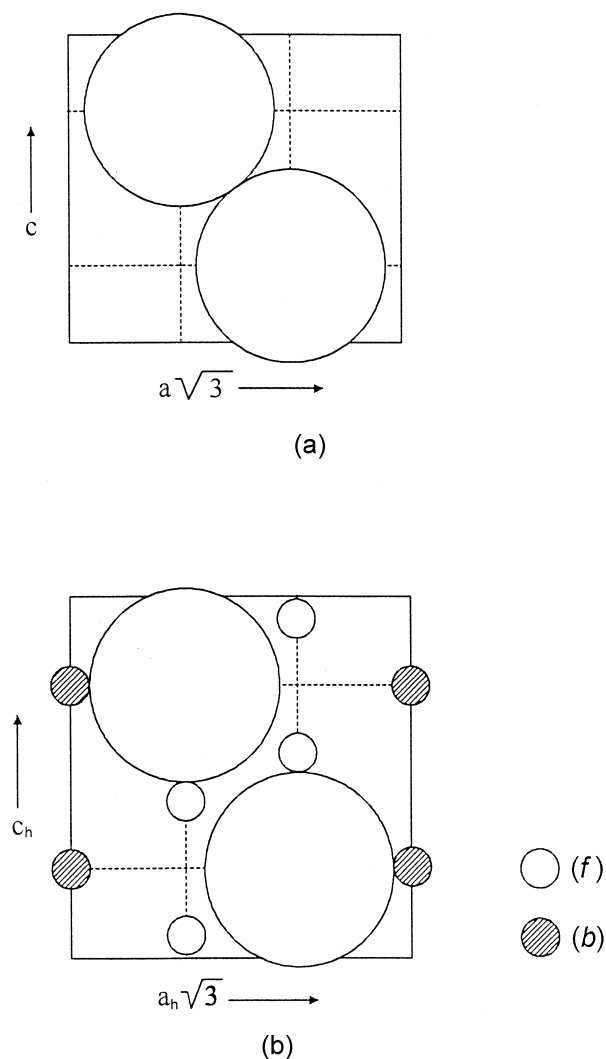


Fig. 2. (a) Schematic position of Gd atoms in the (110) plane of the $\alpha\text{-Gd}$ -unit cell showing the axial ratio $c/a=1.59$. (b) Schematic position of Gd and H atoms in the $(110)_h$ plane of the Na_3As -like substructure showing the axial ratio $c_h/a_h=1.80$. The triangular interstices, i.e. the H-atomic positions (2H (b), $P6_3/mmc$) have been indicated by the hatched circles, the tetrahedral interstices, i.e. the H-atomic positions (4H (f) $P6_3/mmc$) have been indicated by empty circles.

presentation of possible positions of gadolinium atoms is given in Fig. 2a for the (110) plane of the Mg-like unit cell. Analogously, for GdH_3 (if conceived as a Na_3As type structure) a schematic presentation of possible positions for both gadolinium and hydrogen atoms is given in Fig. 2b for the $(110)_h$ plane of the Na_3As -like substructure-unit cell, however, here for the axial ratio corresponding to GdH_3 $c_h/a_h = 1.799$ [$>\sqrt{8/3}$]. With reference to the Gd atomic position (c), four hydrogen atoms occupy the tetrahedral position (f) and thereby it can be understood that upon introducing the H atoms in the α -Gd structure a significant increase of the c_h -axis occurs, causing an increase of the axial ratio c_h/a_h . This explanation obviously applies also to the other late RE-trihydrides exhibiting the Na_3As (sub)structure.

4.2. Relationship between the Na_3As type and the HoH_3 type structures

The relationship between the Na_3As -like unit cell (subscript h) and the HoH_3 -like unit cell (subscript H) is given by:

$$\begin{pmatrix} a_H \\ b_H \\ c_H \end{pmatrix} \approx \begin{pmatrix} 2 & 1 & 0 \\ -1 & 1 & 0 \\ 0 & 0 & 1 \end{pmatrix} \times \begin{pmatrix} a_h \\ b_h \\ c_h \end{pmatrix}$$

The superstructure of GdH_3 is presumed to be isotypical with HoH_3 [6] (i.e. $P\bar{3}c1$, $6\text{Gd}(f)$ with $x=0.3333$; $2\text{H}(a)$; $4\text{H}(d)$ with $z=0.167$; $12\text{H}(g)$ with $x=0.356$, $y=0.328$, $z=0.096$; [11]). In this superstructure the gadolinium atoms also occupy positions of the Mg type structure. The hydrogen atomic positions $2\text{H}(a)$ and $4\text{H}(d)$ ($P\bar{3}c1$) of the

HoH_3 structure, correspond with the triangular atomic positions $2\text{H}(b)$ of the Na_3As ($P6_3/mmc$) structure. However, the octahedral atomic positions $12\text{H}(g)$ of HoH_3 type are not identical with the atomic positions $4\text{H}(f)$ of the Na_3As structure type although the difference is very small. Accordingly, Fig. 2b also approximately characterizes the positions of the Gd and H atoms in the plane $(300)_H$ of the HoH_3 structure type $[(110)_h \approx (300)_H]$.

4.3. Volume and axial ratio c/a of the HoH_3 representatives as function of atomic number

The unit-cell volumes and the axial ratios c/a of the superstructure unit cell (HoH_3 type) are shown for YH_3 and the trihydrides of the late RE elements in Fig. 3 (data from Ref. [4]). The unit cell volume decreases with increasing atomic number. A similar observation was also made for the unit cell volume of the dihydrides REH_2 (CaF_2 type) [8]. The decrease of the unit cell volume with increasing atomic number is ascribed to the corresponding decrease of the atomic radius of the RE elements (lanthanide contraction) [15,16]. On the other hand, the axial ratio c/a of the trihydrides REH_3 increases with increasing atomic number (Fig. 3). The relatively lower axial ratios c_H/a_H of the trihydrides $\text{HoH}_3 \dots \text{TmH}_3$, with respect to those of DyH_3 and LuH_3 , parallels the similarly relatively small values for the axial ratio c/a values of the RE elements $\text{Ho} \dots \text{Tm}$ of the Mg structure type, as shown in Fig. 1.

In the investigated binary system Gd–H, the shortest atomic distances between gadolinium and hydrogen atoms, $d_{\text{Gd-H}}$, are shown for both gadolinium-containing hydrides GdH_2 (CaF_2 type) and GdH_3 (HoH_3 type) in Fig. 4. The

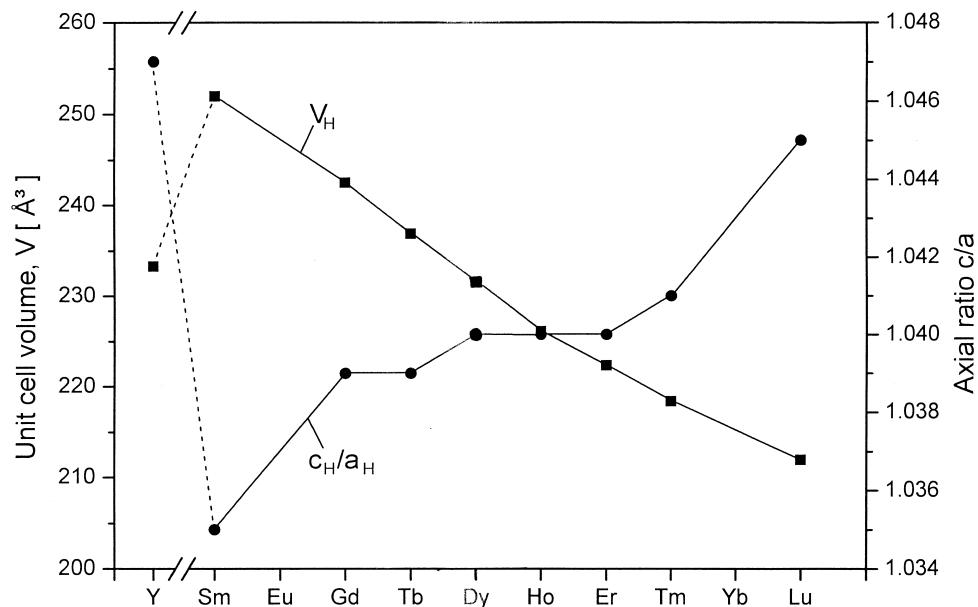


Fig. 3. Unit cell volumes and axial ratios c_H/a_H of yttrium- and late RE-containing trihydrides REH_3 (HoH_3 type) as function of atomic number Z (data from Ref. [4]).

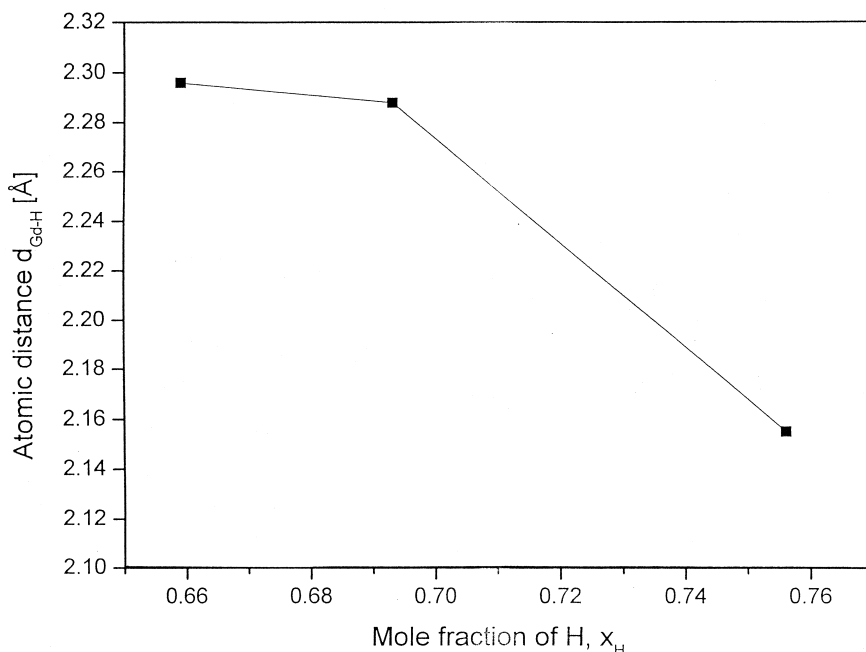


Fig. 4. Shortest atomic distances between gadolinium and hydrogen atoms, d_{Gd-H} , as function of the mole fraction of hydrogen, x_H , for the binary system Gd–H.

d_{Gd-H} -values for the dihydride GdH_2 were calculated from the unit cell parameters given in [8]. Clearly, the shortest atomic distance decreases in the binary system Gd–H with increasing hydrogen content, i.e. with increasing concentration of the s^1 (valence) electrons.

5. Conclusions

(i) The refined unit cell parameters of the trihydride GdH_3 (Ho_3H structure type) are: $a=6.4662(9)$ Å and $c=6.717(3)$ Å.

(ii) The unit cell volume of the late RE trihydrides (HoH_3 type) decreases with increasing atomic number of RE, as a consequence of the decrease of the atomic radius of the RE elements (lanthanide contraction).

(iii) The axial ratio c_H/a_H of the late RE trihydrides (HoH_3 type) increases with increasing atomic number, reflecting more or less the analogous dependence for the axial ratio c/a of the parent late RE element-unit cell (Mg type).

(iv) The shortest distance between gadolinium and hydrogen atoms, d_{Gd-H} , in the intermediate phases of the binary system Gd–H, decreases with increasing hydrogen content.

References

[1] T. Massalski, H. Okamoto, P.R. Subramanian, L. Kacprzak, in: 2nd Edition, Binary Alloys Phase Diagrams, Vol. 2, ASM International,

The Materials Information Society, Materials Park, OH, 1990, p. 1883.
 [2] G.R. Sturdy, R.N.R. Mulford, J. Am. Chem. Soc. 78 (1956) 1083.
 [3] R.N.R. Mulford, G.R. Sturdy, J. Am. Chem. Soc. 77 (1955) 3449.
 [4] P. Villars, Pearson's Handbook, Desk Edition, Crystallographic Data for Intermetallic Phases, ASM International, The Materials Information Society, Materials Park, OH, 1997.
 [5] M. Mansmann, W.E. Wallace, J. de Physique 25 (1964) 454.
 [6] A. Pebler, W.E. Wallace, J. Phys. Chem. 66 (1962) 148.
 [7] Powder Diffraction File (Sets 1-49), International Centre for Diffraction Data, Newtown Square, Pennsylvania, USA, 1999.
 [8] M. Ellner, H. Reule, E.J. Mittemeijer, J. Alloys Comp. 279 (1998) 179.
 [9] N. Mommer, M. Hirscher, F. Cuevas, H. Kronmüller, J. Alloys Comp. 266 (1998) 255.
 [10] K. Yvon, W. Jeitschko, E. Parthé, J. Appl. Crystallography 20 (1977) 73.
 [11] E. Parthé, L. Gelato, B. Chabot, M. Penzo, K. Cenzual, R. Gladyshevskii, in: TYPPIX, Standardized Data and Crystal Chemical Characterization of Inorganic Structures, Vol. 4, Springer Verlag, Berlin, 1994, p. 1385 and 1494.
 [12] T. Hahn (Ed.), Fourth, revised Edition, International Tables for Crystallography, Vol. A, Kluwer Academic Publishers, Dordrecht, 1996.
 [13] Structure Reports for 1955, Vol. 19, N.V.A. Oosthoek's Uitgevers, Utrecht, 1963, p. 259.
 [14] K. Takemura, K. Syassen, J. Physics F: Metal Physics 15F (1985) 543.
 [15] W.B. Pearson, in: The Crystal Chemistry and Physics of Metals and Alloys, Wiley-Interscience, New York, 1972, p. 151.
 [16] J.C. Bailar, H.J. Emeléus, R. Nyholm, A.F. Trotman-Dickenson (Eds.), Lanthanides, Transition Metal Compounds, Comprehensive Inorganic Chemistry, Vol. 4, Pergamon Press, Oxford, 1973, p. 7.